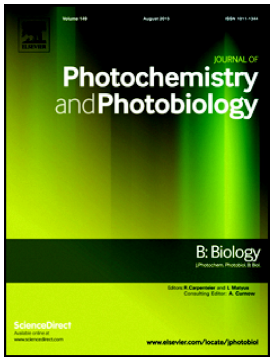


# Light-induced full aromatization and hydroxylation of 7-methoxy-1-methyl-3,4-dihydro-2H-pyrido[3,4-b]indole alkaloid: Oxygen partial pressure as a key modulator of the photoproducts distribution

Fernando Villarruel, M. Paula Denofrio, Federico A.O. Rasse-Suriani, Fernando S. García Einschlag, Tobías Schmidt De León, Rosa Erra-Balsells, Franco M. Cabrerizo

PII: S1011-1344(19)30183-6
DOI: https://doi.org/10.1016/j.jphotobiol.2019.111600
Article Number: 111600
Reference: JPB 111600

To appear in: *Journal of Photochemistry & Photobiology, B: Biology*

Received date: 12 February 2019
Revised date: 12 August 2019
Accepted date: 20 August 2019

Please cite this article as: F. Villarruel, M.P. Denofrio, F.A.O. Rasse-Suriani, et al., Light-induced full aromatization and hydroxylation of 7-methoxy-1-methyl-3,4-dihydro-2H-pyrido[3,4-b]indole alkaloid: Oxygen partial pressure as a key modulator of the photoproducts distribution, Journal of Photochemistry & Photobiology, B: Biology, https://doi.org/10.1016/j.jphotobiol.2019.111600

# Light-induced full aromatization and hydroxylation of 7-methoxy-1-methyl-3,4-dihydro-2H-pyrido[3,4-b]indole alkaloid: oxygen partial pressure as a key modulator of the photoproducts distribution

*Fernando Villarruel,*[a, b] *M. Paula Denofrio,*[a] *Federico A. O. Rasse-Suriani,*[b] *Fernando S. García Einschlag* [b], *Tobías Schmidt De León,*[c, d] *Rosa Erra-Balsells* [c,d] *and Franco M. Cabrerizo* [a,]*

[a] Instituto Tecnológico de Chascomús (INTECH), Universidad Nacional de San Martín (UNSAM) - Consejo Nacional de Investigaciones Científicas y Técnicas (CONICET), Av. Intendente Marino Km 8.2, CC 164 (B7130IWA), Chascomús, Argentina. E-mail: fcabrerizo@intech.gov.ar

[b] Instituto de Investigaciones Fisicoquímicas Teóricas y Aplicadas (INIFTA), CCT-La Plata, Universidad Nacional de La Plata, Diag. 113 y 64 (1900), La Plata, Argentina

[c] Universidad de Buenos Aires. Facultad de Ciencias Exactas y Naturales. Departamento de Química Orgánica. Pabellón II, 3er P., Ciudad Universitaria, (1428) Buenos Aires, Argentina.

[d] CONICET, Universidad de Buenos Aires. Centro de Investigación en Hidratos de Carbono (CIHIDECAR). Facultad de Ciencias Exactas y Naturales. Pabellón II, 3er P., Ciudad Universitaria, (1428) Buenos Aires, Argentina.

* To whom correspondence should be addressed (fcabrerizo@intech.gov.ar)

**ABSTRACT**

Full-aromatic and partially hydrogenated β-carboline (βC) derivatives constitute a group of alkaloids widely distributed in a great variety of living systems. In plants and bacteria, tetrahydro-βCs are the primary product of the Pictet-Spengler enzymatically catalyzed condensation. Tetrahydro-βC skeleton is further modified giving rise to the formation of a vast set of derivatives including dihydro- and full-aromatic βCs. However, in most of the cases, the later processes still remain unclear and other sources, such as photo-triggered reactions, deserve to be explored. In this context, the photophysic and photochemistry of 7-methoxy-1-methyl-3,4-dihydro-2H-pyrido[3,4-b]indole or harmaline (Hlina) in aqueous solution is reported herein. UV-visible absorption and fluorescence emission spectroscopy coupled with multivariate data analysis (PARAFAC), HPLC and HRESI-MS techniques were used for both quantitative and qualitative analysis. The formation singlet oxygen and hydrogen peroxide reactive oxygen species (ROS) was quantified and their role together with the influence of pH and oxygen partial pressure on the photochemical degradation of $HlinaH^+$ was assessed. We report herein the first study on photochemical full-aromatization of a dihydro-βC derivative. These results can shed some light on the βCs biosynthesis and role in living systems.

- - -- - -- - -- - - - - - - - - - - - - - - - - - - - - - - -

**Keywords:** harmaline; harmine; photochemistry; β-carbolines; PARAFAC

## INTRODUCTION

β-carbolines (βCs) constitute a large family of naturally occurring alkaloids structurally related to 9H-pyrido[3,4-b]indole or *nor*harmane (Scheme 1a), showing diverse biological roles such as antitumor, antimicrobial and photodynamic activities [1-16]. The simultaneous presence of both partially hydrogenated (dihydro- and tetrahydro-) as well as full aromatic βCs has been confirmed in a wide range of living species [2]. In particular, 7-methoxy-1-methyl-3,4-dihydro-2H-pyrido[3,4-b]indole also called 7-methoxy-1-methyl-3,4-dihydro-9H-pyrido[3,4-b]indole or harmaline alkaloid (Scheme 1b), and the full-aromatic derivative, 7-methoxy-1-methyl-9H-pyrido[3,4-b]indole or harmine (Scheme 1a) were extracted, for the first time, from *Peganum harmala*, a native species in Africa, the Mediterranean area, Middle East and South Asia. Abundance of these alkaloids showed great variances between biological species [17]. *Banisteriopsis caapi*, a plant originally from Amazons, contains quite high levels of dihydro-βCs (up to 0.05 – 1.95 % of dry-mass) [18]. Harmaline and other dihydro- and tetrahydro-derivatives together with several full aromatic-βCs were also found in the cuticle of two species of fluorescent scorpions (*Centruroides vittatus* and *Pandinus imperator*) [19]. Moreover, partially hydrogenated βCs are also normal constituents of human body tissues and corporal fluids such as plasma, pineal glands and other photosensitive tissues/organs including skin as well as the retina and the crystalline of eyes [20, 21].

To date, information regarding βCs' biosynthesis is still incomplete and the chemical processes involved need to be studied. The formation of tetrahydro-βCs would involve a catalyzed Pictet-Spengler condensation from tryptophan and aldehydes. The type and number of enzymes involved in this process differ from one organism to another. In plants, strictosidine synthase (STR) catalyzes the condensation reaction between tryptamine and secologanin giving rise to the formation of the corresponding tetrahydro-βC derivative [22-25]. On the contrary, different multi-functional enzyme families would be responsible for the biosynthesis of these alkaloids in several microorganisms [26, 27]. In particular, microbial homodimeric enzyme McbB,[28] isolated from *Marinactinospora thermotolerans*, catalyze the Pictet-Spengler reaction between *L*-tryptophan and oxaloacetaldehyde [26].

Tetrahydro-βC skeleton can be further modified yielding a vast set of derivatives, such as dihydro-, epoxy-, keto-, isomeric hydroxy-, and/or full aromatic βCs. The formation of these compounds may be enzymatically catalyzed. For instance, in microbial agents, McbB complex would also contribute to the formation of decarboxylated and full aromatic βCs, respectively [26]. Other enzymatic (*i. e.*, cytochrome *P*-450cam mediated) and/or non-enzymatic processes can also play important roles [29, 30]. However, in most cases, oxidation and/or full-aromatization processes still remain unclear. Furthermore, taking into account the presence of these alkaloids in aerial organs

exposed to sun light (*e. g*. leaves and stems) photochemical pathways need to be further explored. [31]

We report herein the first photochemical study of harmaline (Hlina), in aqueous solution. In the pH-range 2 - 12, Hlina shows one dominant acid-base equilibria with p$K_a$ = 10 (Scheme 1b) [32-34]. It has been well stablished that, in general, each acid-base species of these alkaloids can show quite distinctive chemical and photochemical properties in solution [9, 10, 35-42]. Besides, in some cases, these properties depend on the level of dissolved oxygen [38-40, 43]. Thus, in the present study, the effects of pH and oxygen partial pressure on the photophysic and photochemistry of Hlina were investigated.

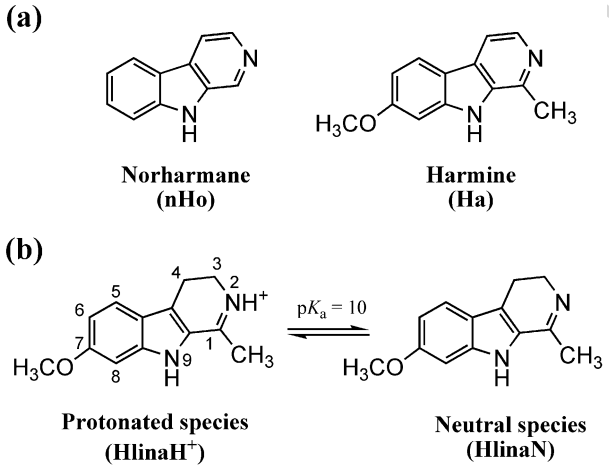


**Scheme 1. (a)** Chemical structure of two representative full-aromatic βC alkaloids. **(b)** Acid-base equilibria and chemical structure of harmaline species observed in aqueous solution in the pH range 2 –13.5.

## EXPERIMENTAL

*General*. *nor*harmane, harmine and harmaline (> 98%, Sigma-Aldrich) $H_2O$ and $D_2O$ stock solutions were prepared according to the procedure described elsewhere [38, 39]. HPLC and HRESI-MS analyses of Harmalina solutions reveal a small percentage of harmine as impurity (< 2%).

*Irradiation set-up*. Air-equilibrated or $N_2$-saturated βC aqueous solutions were irradiated at 350 nm, in 1 cm quartz cells at room temperature with a Rayonet RPR lamp (bandwidth ~ 15 nm, Southern N.E. Ultraviolet Co.). Oxygen-free solutions were obtained by purging with $N_2$ gas (purity 5.0) for 30 min.

*UV-visible analysis.* Electronic absorption spectra were recorded on a Perkin-Elmer lambda 25 spectrophotometer, in 1 cm path length quartz cells, at room temperature.

*High-Performance Liquid Chromatography (HPLC)*. Photochemical reactions were monitored and quantified using *(i)* a Waters instrument with a 1525 binary Pump controller and a 2475 multi-λ fluorescence detector (HPLC set-up I) [40] and *(ii)* a Shimadzu equipment: solvent delivery module LC-20AT, on-line degasser DGU-20A5, communications bus module CBM-20, auto sampler SIL-20A HT, column oven CTO-10AS VP and photodiode array detector SPD-M20A (HPLC set-up II)

[44]. Stationary phase: GracePrevail RP18 (250 x 4.6 mm, 5 μm). Mobile phase: a 50/50 (v/v) mixture of formic acid (Sigma-Aldrich) aqueous solution (0.08% (v/v), pH 3.2) and MeOH (J. T. Baker). Flow rate: 1 mL $min^{-1}$.

*Quantum yields of βCs' photodegradation, $\Phi_R$:* Values were determined according the procedures and equations described elsewhere [38, 40].

*Detection and quantification of $H_2O_2$.* An enzymatic Glycemia Kit (Wiener Lab.) was used for $H_2O_2$ detection. The levels of $H_2O_2$ produced upon irradiation were quantified after reaction with 4-aminophenazone and 4-hydroxybenzoate. Minor changes were introduced to the general procedure previously described [39, 40]. Briefly, 1.25 ml of irradiated solution (UVA, 350 nm) were mixed with 1.50 ml of the colorimetric reagent and absorbance at 505 nm ($A^{505nm}$) was measured after 40 min of incubation at room temperature. Calibration curve was obtained from aqueous $H_2O_2$ solutions prepared from commercial standards. A $\varepsilon^{H_2O_2}$ value of 17.7 $M^{-1}cm^{-1}$ (at 254 nm) was used to determine the [$H_2O_2$] in each of the standar solutions.

Generaly, the photodegradation of βCs yields photoproducts exibiting non-negligible absorption coefficients around 450-550 nm. Thus, to avoid interferences, another set of irradiated solutions was incubated with catalase (final concentration 10 U/μl) prior the incubation with the colorimetric reagents for $H_2O_2$ determination. The comparison of the latter control experiments with data obtained from the non-enzymatically-treated samples allowed us to conclude whether the obtained signals at $A^{505nm}$ may be ascribed to the formation of $H_2O_2$ or not.

*Fluorescence emission. (i)* Steady-state fluorescence measurements were performed using a Fluoromax4 (HORIBA Jobin Yvon) instrument. Corrected fluorescence spectra were recorded in a 1 cm x 1 cm path lengths quartz cell at room temperature. Fluorescence quantum yields ($\Phi_F$) were determined from the corrected fluorescence spectra, integrated over the entire emission profile and were calculated as the average of $\Phi_F$ values obtained using different excitation wavelengths over the entire range of the lowest-energy absorption band. Standards used were quinine sulfate (in 1N $H_2SO_4$ aqueous solution, $\Phi_F$ = 0.52 ± 0.02) [45] and *nor*harmane (in air-equilibrated pH 4.8 aqueous solution, $\Phi_F$ = 0.70 ± 0.05) [38, 39]. Inner filter effects were avoided by keeping the absorbance of the solutions (at the excitation wavelengths) below 0.10. *(ii)* Fluorescence lifetimes, $\tau_F$, were obtained from time-resolved fluorescence experiments performed on a single-photon-counting FL3 TCSPC-SP (HORIBA Jobin Yvon) spectrofluorometer. Two different NanoLED sources centered at 341 nm and 388 nm were used for excitation whereas emission decays were monitored at the corresponding emission maxima of each emitting species (*vide infra*). Under our experimental conditions, all $\tau_F$ were obtained from mono-exponential decays observed after deconvolution from the instrument response function signal [7].

*Quantum yields of photosensitized singlet oxygen ($^1O_2$) production*. Equipments and procedures were previously described in detail [38, 39]. Briefly, in these experiments a pulsed Nd-YAG laser was used as excitation source ($\lambda_{exc}$ = 355 nm) and the signal at the 1270 nm $^1O_2$ phosphorescence was sensed by a cooled Germanium detector. $\Phi_\Delta$ values were determined by comparing the magnitude $^1O_2$ phosphorescence signals (extrapolated at zero time) produced upon one-photon excitation of deuterated aqueous solutions of βCs to that produced by perinaphthenone-2-sulfonic acid ($\Phi_\Delta$ = 0.97 ± 0.05) [46] used as standard.

*Parallel factor analysis (PARAFAC).* PARAFAC analysis was conducted using MATLAB R2015b (Mathworks, Natick, MA) with the N-way toolbox (http:models.klv.dk/source). Three way data sets were constructed from the excitation emission matrices (EEM) recorded during each irradiation experiment. The required preprocessing steps were adopted to account for both primary and secondary inner filter effects (IFE) and also to minimize the influence of scattering effects [47, 48]. Briefly, the absorption espectra of the samples were used for correcting the attenuation of fluorescence signals due to IFE, subsequently the EEM of a control (Milli-Q water) was subtracted from each sample EEM, and finally Rayleigh and Raman scattering signals were removed according to the protocol described by Bahram *et. al.* [49]. PARAFAC models with two to five components were computed for each set of EEMs. Non-negativity constraints were applied to all factors in the three modes, thus allowing only chemically relevant results. The determination of the correct number of factors, required to properly decompose each data set, was assessed by the inspection of the physical sense of spectral loadings, the evaluation of the distribution of residuals and the application of the core consistency diagnostic test. [48]

*HRESI–MS analysis*. High resolution electrospray ionization (HRESI) mass spectrometry (MS) analyses were performed in positive and negative ion modes using the mass spectrometer Q Exactive from Thermo Scientific (USA). Acquisition parameters were: flow rate: 5000 µL/min, scan range: 55 to 800 m/z, resolution: 140,000, sheath gas flow rate: 30 CFH, aux. gas flow rate: 0 CFH, spray voltage: 3.50 kV, S lens voltage 50 V, capillary temp: 320 ºC, aux. gas heater temp: 30 ºC and acquisition time: 0.5 min. Fresh water solutions of the commercial analytes (harmaline; harmine) were used as references for the direct infusion and analysis; the pH of these solutions was the same as that of the monitored irradiated solution. Molecular formula and monoisotopic molecular weight were obtained. Neutral compounds were detected in the positive and negative ion modes, as protonated $[M + H]^+$ and deprotonated species $[M - H]^-$, respectively. Then calculated monoisotopic photoproducts m.w. and the probable molecular structure are discussed below.

## RESULTS

*UV–visible absorption and fluorescence emission spectroscopy.*

UV-visible absorption and fluorescence excitation and emission spectra of harmaline have been well described and characterized [32, 34, 50]. Briefly, in aqueous media, both acid-base species of harmaline show a high molar absorption coefficient in the UVA region of the electromagnetic spectrum ($\varepsilon \sim 1.5 \times 10^4$ $M^{-1}$ $cm^{-1}$). In particular, the protonated species, $HlinaH^+$, shows a clear bathochromic shift with molar absorption coefficient, $\varepsilon$, values up to $2.0 \times 10^4$ $M^{-1}$ $cm^{-1}$ in the visible region (Figure 1, filled circles). The latter is the dominant species (> 99%) under physiological pH conditions.

Emission fluorescence spectra of both protonated ($HlinaH^+$) and neutral (HlinaN) species of harmaline were recorded (Figure 1). Under both pH conditions only one emitting band, centered at ~ 484 nm, was observed. The latter band has been univocally ascribed to the emission of photoexcited $HlinaH^+$ ($[HlinaH^+]^*$). Note that, despite the almost negligible emission recorded, $[HlinaH^+]^*$ is still the only emitting species even under alkaline conditions (pH 13.1). This fact can be accounted by considering the small fraction (< 0.1%) of $HlinaH^+$ present in the solution at this pH capable to absorb the incident light, in combination with a null $\Phi_F$ value of the photoexcited neutral species [HlinaN]* (see below).

The corresponding quantum yields of fluorescence ($\Phi_F$) are listed in Table 1. For comparative purpose, data reported for the full-aromatic related βC, Ha, have also been included. [37] Briefly, harmaline showed lower $\Phi_F$ values than Ha (this fact is more evident under alkaline conditions), and no oxygen dependence was observed in any case. In particular, $HlinaH^+$ showed a larger $\Phi_F$ value than HlinaN (*i.e.*, 0.40 ± 0.03 and 0.01 ± 0.01, respectively). These results match with those previously reported for harmaline under similar experimental conditions [34, 50]. Furthermore, $\Phi_F$ reported herein for HlinaN is the same, within the experimental error, than that previously reported for harmaline in acetonitrile (< 0.03 ± 0.03). [33]

These findings suggest that, on the contrary to what have been reported for almost all full-aromatic βCs, the basic character of N(2) in the HlinaN ring shows no accountable differences, neither in the electronic ground nor in the excited states. Thus, the fast protonation typically observed for full-aromatic βCs would not take place in the case of this dihydro-derivative (HlinaN).

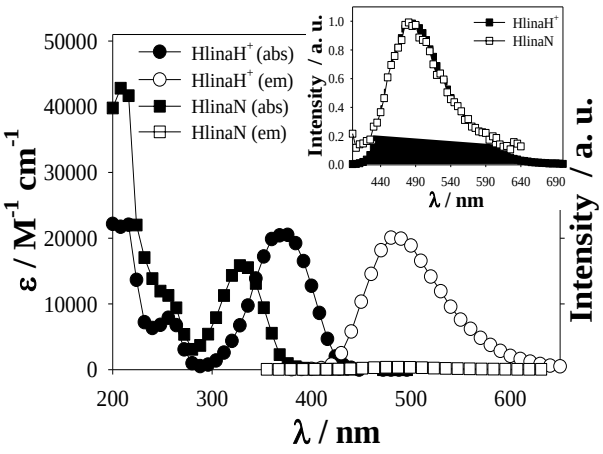

**Figure 1.** UV–visible absorption (filled symbols) and emission (empty symbols) spectra of $HlinaH^+$ (circles) and HlinaN (squares) species of harmaline in aqueous solution (pH 4 and 13.1, respectively). *Inset:* normalized emission spectra recorded under both pH conditions.

*Photosensitized singlet oxygen $^1O_2$ production ($\Phi_\Delta$).*

The capability to photosensitize $^1O_2$ formation by full aromatic βCs and its dependence on the nature of the environment have been well established. In particular, in aprotic organic solvents full aromatic βCs show $\Phi_\Delta$ values ranging from 0.31 to 0.40 [51]; whereas values recorded in aqueous media have shown to be considerably lower (*i.e.*, $\Phi_\Delta$ values of ~ 0.08, with the exception of Ha showing a $\Phi_\Delta$ value of 0.22) [11, 36, 38-40, 43]. In most cases, oxygen partial pressure enhances the efficiency of $^1O_2$ production [39, 43]. However, dihydro-βCs have not been carefully investigated yet.

In this context, $\Phi_\Delta$ values were determined herein for the two acid-base species of harmaline in aqueous solution as a function of ambient oxygen partial pressure in: air-equilibrated- and $O_2$-saturated solutions (Tables 1). These results indicate that both species are rather poor or null $^1O_2$ photosensitizers ($\Phi_\Delta$ values fall within the experimental error). The same trend was observed in acetonitrile ($\Phi_\Delta < 0.05 \pm 0.05$) suggesting the absence of typical solvent-effect shown by other βC alkaloids. [33] The lack of $^1O_2$ production is in connection with the fact that triplet formation for harmaline, even under $N_2$-saturated conditions, was undetectable. Thus, other deactivation pathways such as fluorescence emission (see above) and non-radiative processes [33] would be more efficient than the intersystem crossing (ISC) to populate the triplet state.

**Table 1.** Photochemical and photophysical parameters determined upon one-photon excitation of harmaline (Hlina) and harmine (Ha) in aqueous solution, under acidic and alkaline conditions.

| | **Ha** | | | | **Hlina** | |
|---|---|---|---|---|---|---|
| **p$K_a$ ($S_0$)** | p$K_a^{N-2}$: 7.5 | | | | p$K_a^{N-2}$: 9.7, [c] 9.54 (± 0.03) | |
| **pH** | 4.0 | 10.0 | | | 4.0 | 13.1 |
| **Species at $S_0$** | $HaH^+$ | HaN | | | $HlinaH^+$ | HlinaN |
| **$\lambda_{abs}$ / nm** | 355 | 335 | | | 372 | 330 |
| **$\varepsilon(\lambda)$ / $10^3$ $M^{-1}$ $cm^{-1}$** | 7.85 | 4.55 | | | 20.65 | 15.95 |
| **Species at $S_1$** | $[HaH^+]$* | [HaN]* | $[HaH^+]$* | [f] [HaZ]* | $[HlinaH^+]$* | [g] $[HlinaH^+]$* |
| **$\lambda_{fluo}$ / nm** | 417 | ~356 | 417 | ~500 | 484 | 484 |
| **[d, e] $\Phi_F$ ($N_2$-sat)** | [a] 0.47 ± 0.05 | [a] 0.39 ± 0.05 | | | 0.37 ± 0.04 | 0.01 ± 0.01 |
| **[d, e] $\Phi_F$ (air)** | [a] 0.49 ± 0.05 | [a] 0.38 ± 0.05 | | | 0.40 (± 0.03); [c] 0.46 and [d] 0.32 (± 0.02) | 0.01 ± 0.01 |
| **[d] $\Phi_F$ ($O_2$-sat)** | [a] 0.47 ± 0.05 | [a] 0.36 ± 0.05 | | | 0.37 ± 0.04 | 0.01 ± 0.01 |
| **$\tau$ / ns** | [a, b] 7.05 ± 0.05 | [b] 0.44 ± 0.02 | [b] 6.95 ± 0.05 | --- | 5.87 ± 0.04 | --- |
| **$\Phi_\Delta$ (air)** | [a] 0.22 ± 0.02 | [a] 0.13 ± 0.01 | | | 0.02 ± 0.01 | 0.003 ± 0.002 |
| **$\Phi_\Delta$ ($O_2$-sat)** | [a] 0.24 ± 0.02 | [a] 0.13 ± 0.01 | | | 0.03 ± 0.01 | 0.003 ± 0.002 |
| **$\Phi_R$ (air)** | [a] $3.73 \times 10^{-3}$ | --- | | | $1.12 \times 10^{-3}$ | --- |
| **$\Phi_R$ ($N_2$-sat)** | [a] 0 | --- | | | $3.16 \times 10^{-3}$ | --- |
| **$\Phi_{H_2O_2}$ (air)** | $0.84 \times 10^3$ | --- | | | nd | --- |
| **$\Phi_{H_2O_2}$ ($N_2$-sat)** | nd | --- | | | nd | --- |

[a, b, c and d] From Ref [[39]], [[36]], [[34]] and [[50]], respectively. nd = not detected. [e] $\Phi_F$ are the means of values obtained using excitation wavelengths over the entire range of the lowest-energy absorption band. Independent data sets determined in separate experiments against different standards were indistinguishable from each other. [f] HaZ represents the zwitterionic species of Ha. [g] Photoexcited $HlinaH^+$ ($[HlinaH^+]$*) is the emitting species most probably due to a minor

contribution of the small fraction of HlinaH$^+$ (< ~0.1%) capable to absorb the incident light, present in the solution under this pH condition.

*Steady-State Irradiation and photochemical degradation of HlinaH$^+$.*

The photostability of HlinaH$^+$, main acid-base species under physiological pH, was studied in aqueous solutions (pH 4.0 - 7.4) subject to steady-state UVA-irradiation. Briefly, experiments performed with air-equilibrated solutions showed significant changes in the absorption spectra during the elapsed irradiation time (Figure 2a). In contrast to the general behavior of full aromatic βCs, a photochemical reaction was also observed under $N_2$-saturated atmosphere (Figure 2b). The pattern and extent of the changes observed were significantly different. Such differences are better represented in Figures 2c where normalized experimental difference (NED) spectra are compared. The largest differences are observed in the spectral region ranged between 200 nm and 325 nm. Briefly, photoproduct/s obtained under air showed absorption maxima at *c.a.* 225 nm and 290 nm (black lines); whereas photoproduct/s formed in $N_2$-saturated solution showed two absorption maxima at *c.a.* 240 nm and 320 nm (red lines). The latter photoproduct/s exhibit a pattern consistent with that corresponding to the full aromatic βCs HaH$^+$ (see below).

Under both atmosphere conditions, HPLC analysis showed a decrease in HlinaH$^+$ concentration. Profiles followed a pseudo zero-order kinetics in the time-window investigated (Figure 2d). Rates of reactant disappearance of 0.022 ± 0.005 μM min$^{-1}$ and 0.063 ± 0.002 μM min$^{-1}$ were observed under air-equilibrated and $N_2$-saturated conditions, respectively. The corresponding quantum yields of HlinaH$^+$ disappearance ($\Phi_R$) were calculated taking into account the incident photon flux and the absorbance of HlinaH$^+$ at 350 nm (Table 1). Moreover, under anaerobic condition the formation of Ha was confirmed by the chromatographic peak at Rt = 11 min (Figure SI.1). It is noteworthy that the rate of Ha formation was ~ 6 times lower than that of HlinaH$^+$ consumption. This fact suggests that the formation of additional photoproducts would take place (see below).

Complementary chromatograms recorded with HPLC set-up II, monitored at four different absorption wavelengths (220, 280, 320 and 372 nm) clearly show a distinctive pattern of photoproduct distribution when comparing the progress of the photochemical reaction conducted under both atmospheres (Figures SI.2 - SI.5). Briefly, in air-equilibrated conditions beside the decrease of the reactant (HlinaH$^+$) the appearance of a complex photoproducts mixture with, at least, four components (detected at Rt of 3.1, 3.8, 5.2 and 6.8 min) was observed. On the other hand, photodegradation of HlinaH$^+$ performed in $N_2$-saturated aqueous solution gives rise to the appearance of the full-aromatic derivative Ha together with, at least, three components detected at Rt of 3.5, 4.5 and 6.0 min. According to the UV-visible spectra recorded with the photo-array detector (Figure SI.6), photoproducts obtained in air-equilibrated solutions mainly absorb at *c.a.* 280 nm. This feature is compatible with indole/indolenine-like structures (see below), with minor contribution at *c.a.* 330

and 350 nm. On the contrary, under $N_2$-saturated conditions the mixture of photoproducts showed an important absorption around 320 nm, with contributions at *c.a.* 250 and 280 nm. This pattern is compatible with full-aromatic βC-like structures (see below).

The trend and extent of the photochemical degradation of $HlinaH^+$ observed in irradiated neutral (pH 7.4) solutions were the same, within the experimental error, to that observed under acidic conditions (Figures 2c, 2d and SI.11). These results were expected due to the fact that $HlinaH^+$ is the dominant species (> 99%) in solution of pH values ranging from 2 to 8.

The production of $H_2O_2$ upon UVA irradiation of several βCs has been reported [38-40]. Thus, the presence of $H_2O_2$ upon irradiation of air-equilibrated solutions of $HlinaH^+$ ($[HlinaH^+]_0$ = 25 µM, pH 4.0) was investigated under the same experimental conditions as those used for $\Phi_R$ determination. The results showed undetectable $H_2O_2$ photosensitized production (Table 1 and Figure SI.7). This fact represents a major difference with respect to the full aromatic βCs.

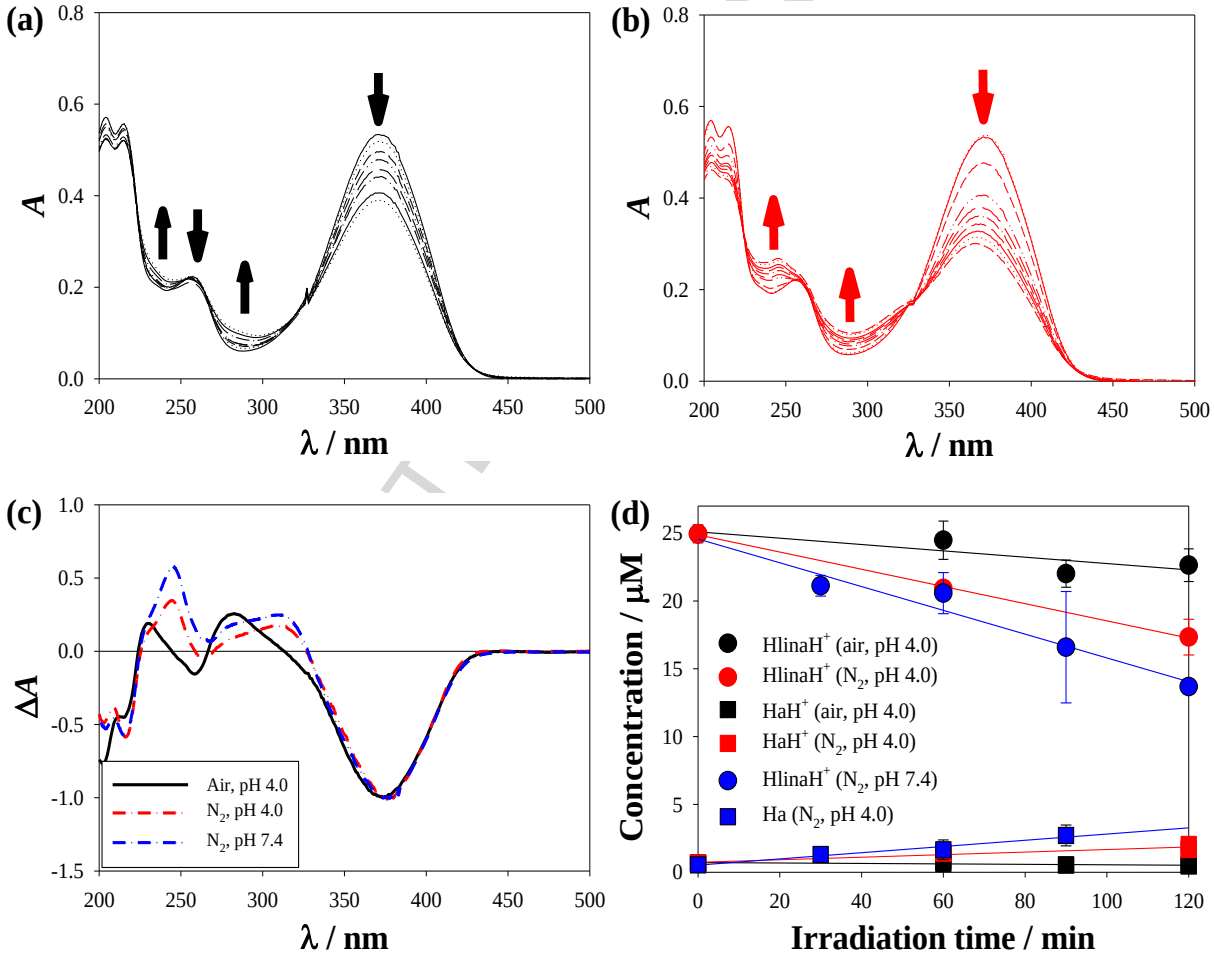


**Figure 2.** Evolution of the UV-visible absorption spectra of **(a)** air-equilibrated and **(b)** $N_2$-saturated aqueous solution of $HlinaH^+$ (25 µM), as a function of the irradiation time (0, 15, 30, 45, 60, 75, 90 and 120 min). **(c)** Comparison of Normalized Experimental Difference (NED) spectra recorded under different atmosphere and pH conditions. **(d)** Evolution of $HlinaH^+$ (circles), $HaH^+$ (squares) concentrations in air-equilibrated (black) and $N_2$-sat. acidic (red) and $N_2$-sat. neutral (blue) conditions as a function of the elapsed 350 nm irradiation time. βC concentrations were assessed by HPLC analysis using a fluorescence detector (excitation/emission channels 320/420 nm and 370/450 nm were particularly used to detect Ha and Hlina, respectively).

*PARAFAC analysis: fluorescence excitation-emission matrices of irradiated HlinaH$^+$ aqueous solution.*

Fluorescence excitation-emission matrices and parallel factor analysis (PARAFAC) were used to further characterize the behavior of HlinaH$^+$ solutions upon irradiation. Brielfy, the results obtained under $N_2$-saturated atmosphere confirm the photochemical generation of Ha during the irradiation of HlinaH$^+$ solutions. This is accounted by the appearance of an important emission signal centered at Ex/Em ~ 315 nm/415 nm (Figures 3a and SI.8) not observed in the presence of dissolved oxygen (Figures 3b and SI.9). Moreover, PARAFAC algorithm, used to decompose the three way arrays obtained by stacking the EEMs recorded under both atmosphere conditions, was able to identify and resolve the concentration profiles corresponding to the two major contributions. Figure 4 shows that the resolved excitation and emission spectra fully match with those corresponding to HlinaH$^+$ and the full-aromatic derivative, Ha. Scores with the relative contribution of each species are shown in Figure SI.10. The trend and extent obseved on irradiated air-equilibrated neutral (pH 7.4) solutions were the same, within the experimental error, to that observed under acidic conditions (Figure SI.10).

In contrast, a carefull inspection of the EEM obtained under air-equilibrated atmosphere suggests the appearance of a rather small but non negligible emission signal centered at Ex/Em ~ 290 nm/330 nm (Figure 3d). This behavior was not observed in the absence of dissolved oxygen (Figure 3c). It is important to note that, despite the relatively small intensity of these signals in comparison with those recorded for HlinaH$^+$, the latter increase in the emission was recorded whithin a range of excitation wavelengths for which the absorbance of HlinaH$^+$ is practically null. Therefore, any variation in the total counts recorded by the spectrofluorometer when the excitation monochromator scanned from 270 to 310 nm should be ascribed to chemical species different from HlinaH$^+$ reactant. Moreover, PARAFAC algorithm suggests that, in the presence of dissolved oxygen, the contribution of a third factor, centered at Ex/Em 290 nm/330 nm (see inset to Figure 4), increases with irradiation time. Hence, despite the profiles obtained for the third factor are noisy and may be subject to some degree of correlation (specially for the spectral ranges where HlinaH$^+$ exhibits much higher emission intensities) their spectral location in both excitation and emission modes strongly suggests the formation of indole-like structures and points to the loss of the extra double bond conjugation present in HlinaH$^+$ upon irradiation under air-equilibrated atmosphere.

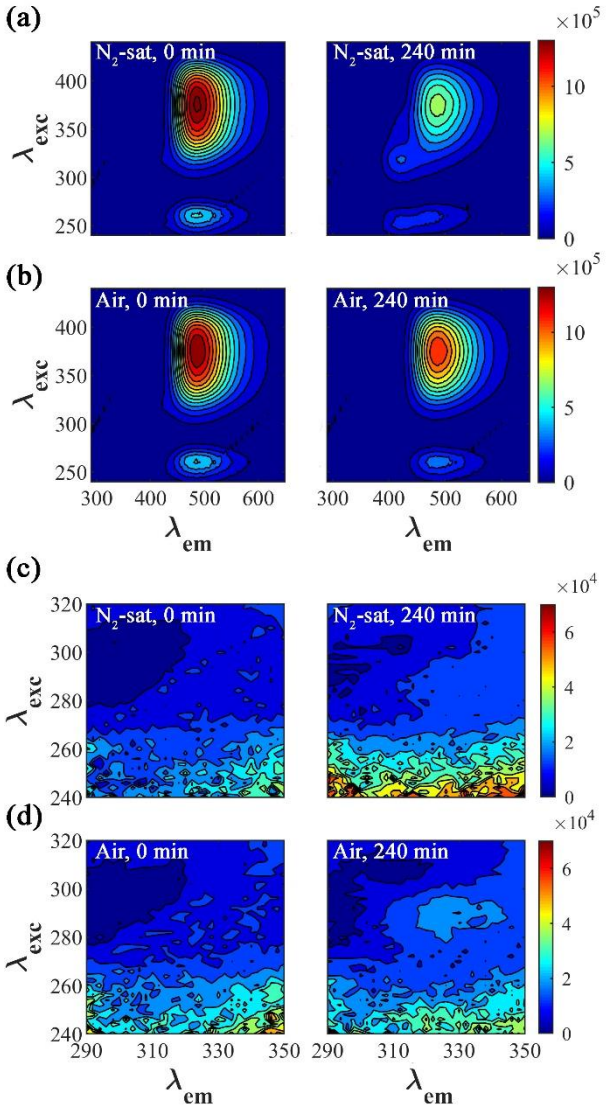


**Figure 3.** Fluorescence excitation-emission matrices obtained for $HlinaH^+$ under air-equilibrated and $N_2$-saturated atmosphere: **(a)** and **(b)** $[HlinaH^+]_0$ = 50 µM; **(c)** and **(d)** $[HlinaH^+]_0$ = 145 µM.

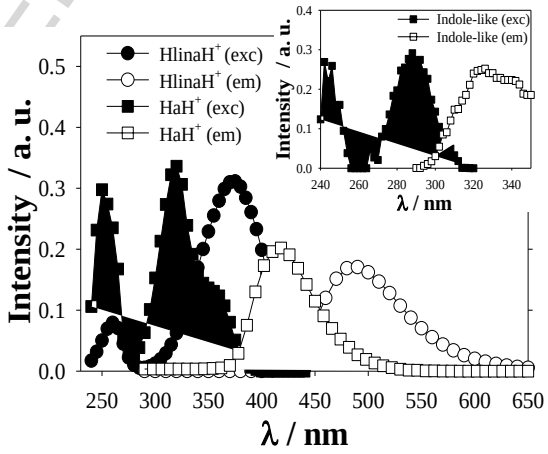


**Figure 4.** Normalized excitation and emission spectra of $HlinaH^+$ and the photoproducts generated upon irradiation obtained by PARAFAC performed with the two tensors obtained from fluorescence excitation – emission matrix (EMM) recorded under both atmosphere conditions (air-equilibrated and $N_2$-saturated solutions). *Inset:* data obtained from EEM recorded at low excitation-emission wavelengths (Figures 3c and d).

*HRESI-MS analysis.*

Composition changes of $HlinaH^+$ solutions of pH 4.0, irradiated (0, 120, 180 and 240 min) under both air-equilibrated and $N_2$-saturated atmospheres, were monitored by HRESI-MS. In the presence of oxygen, Hlina as $[Hlina+H]^+$ species behaved as a quite stable compound. After 180 min the irradiated solution showed the formation of a photoproduct at m/z = 231 that includes oxygen in its structure (Figure 5c; Hlina peak at m/z = 215, as $[M+H]^+$ and the photoproduct peak at m/z = 231, as $[M+H]^+$, then m.w. = 230). The strong electrophilic character of the pyrido[3,4b] doble bound constituent of the indolic moiety, enhanced because of the protonation of the pyridinic N(2) and the resulting positive charge on it, can explain the $O_2$ attact to this position yielding, as stable derivative to detect by ESI MS method, the 4a,9a-epoxy-harmaline derivative (Scheme 2a) and/or the 4a-hydroxyindolenine derivative (Scheme 2b) (both with m.w. = 230). In negative ion mode the corresponding peak at m/z = 229 was observed (Figure 5d; Hlina peak at m/z = 213, as $[M - H]^-$ and the photoproduct peak at m/z = 229, as $[M-H]^-$, then m.w. = 230). Schemes 2c and d show the possible structures for the deprotonated species detected. On the contrary, when irradiation was conducted under $N_2$-saturated atmosphere, the formation of a photoproduct with m/z 213 was detected, in positive ion mode. After 240 min, the irradiated solution showed a ratio aprox 70:100 among the photoproduct (m/z 213) and Hlina (m/z 215) (Figure 5a). Clearly under this experimental conditions the full aromatization of Hlina takes place and harmine is produced (positive ion mode, sepcies detected as $[M+H]^+$, photoproduct with m/z 213, then m.w. 212). Results obtained in negative ion mode are similar (Figure 5b; negative ion mode, species detected as $[M-H]^-$, photoproduct with m/z 211, then m.w. 212). The production of harmine as stable photoproduct suggests that, simultaneously to this oxidative-dehydrogenation process, a reductive hydrogenation may be opperating specially if the dehydrogenation would involve a 2 steps homolytic C-H breaking bond (radical species formation). In that conditions additional products (*e. g.*, 1,2-dihydrogenated harmaline, harmaline dimers, trimers, etc.) should be formed and detected at least by HPLC analysis. In connection with this topic, the results obtained have been included in Figures SI.2-SI.5 and previously discussed. As Ha shown to be the photoproduct formed in higher yield, may be dehydrogenation should be taking place as a concerted hydrogen elimation process as well.

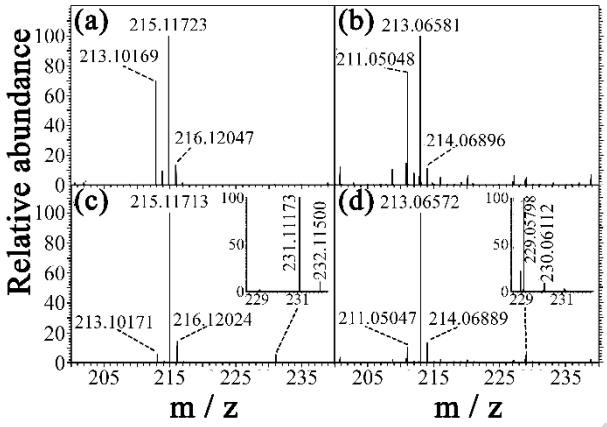


**Figure 5.** HRESI mass spectra of irradiated $HlinaH^+$ aqueous solution (pH, 4.0; irradiation time = 240 min; atmosphere, (a) and (b) $N_2$, (c) and (d) air; ion mode, (a) and (c) positive; (b) and (d) negative. Base peak absolute intensity: (a) 6.56 x $10^7$, (b) 5.56 x $10^6$, (c) 2.87 x $10^8$ (*Insert:* 1.46 x $10^7$), (d) 2.35 x $10^7$ (*Insert:* 1.78 x $10^6$) a. u.; (c) and (d) show the presence of Ha as impurity (< 2%) of Hlina.

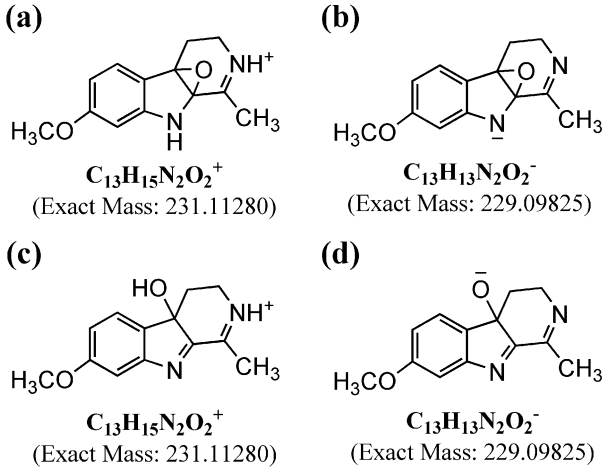


**Scheme 2.** HRESI-MS analysis. Proposed structures for the ions formed by the photoproducts present in the irradiated Hlina acidic air-equilibrated aqueous solution; **(a)** and **(b)** positive ion mode, **(c)** and **(d)** negative ion mode.

## CONCLUSIONS

The present work provides qualitative and quantitative data concerning the photophysical and photochemical behavior of harmaline alkaloid in aqueous solution under both acidic and alkaline conditions. It is worth to mention that, although there are several articles reported in the field, we focused our attention on unresolved key aspects that needed clarification. Thus, values of quantum yield of singlet oxygen ($\Phi_\Delta$) and hydrogen peroxide ($\Phi_{H2O2}$) production here reported indicate that, under the whole pH-range investigated (3.0 < pH < 13.1), this alkaloid has a quite small or null capability of photoinduced ROS production. The pH-dependence of Hlina fluorescence quantum yields ($\Phi_F$) was also investigated. Data show that the protonated species $HlinaH^+$ is a rather efficient fluorophore.

In addition, the photochemical degradation of $HlinaH^+$ was, to the best of our knowledge, studied for the first time. In this context, we demonstrate herein that, upon photoexcitation, $HlinaH^+$ leads to the formation of different photoproducts and that oxygen partial pressure strongly modulates the extent of the reaction as well as the type of photoproduct generated (Scheme 3). This study

provides relevant information that may contribute to further understand or consider additional pathways for the *in vivo* synthesis and/or photochemical modification of βCs.

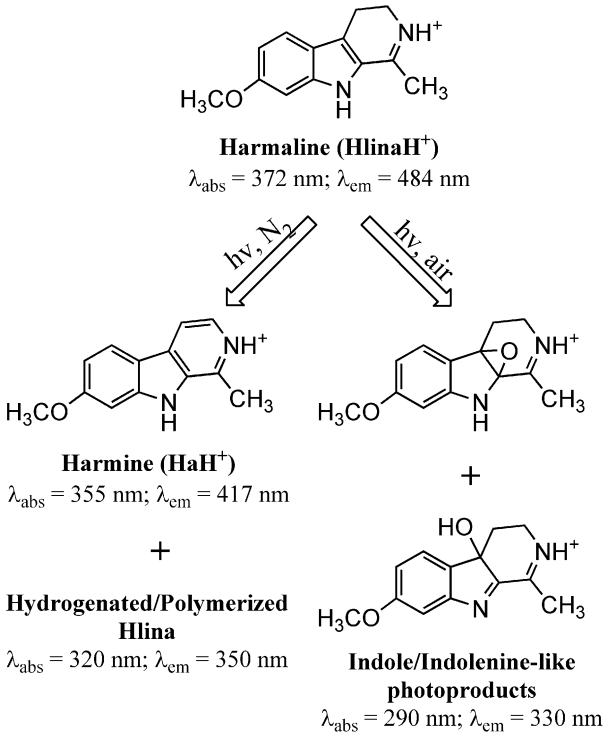


**Scheme 3.** Photochemical reactions proposed for the photodegradation of $HlinaH^+$ alkaloid in aqueous solution (pH 4.0), under different atmospheres.

## ACKNOWLEDGEMENTS

The present work was partially supported by UBA (2018-00110BA), ANPCyT (PICT 2015-0374, 2016-0370 and 2016-0130). F. D. V. and T. S. D. L. thank ANPCyT and CONICET, respectively, for their doctoral research fellowships. MPD, SGE, REB and FMC are research members of CONICET (Argentina). Authors deeply thank Carlos G. Alberici for photo-reactors designs and technical assistance, and Dr. P. R. Ogilby for his contributions in singlet oxygen experiments performed at Centre for Oxygen Microscopy and Imaging, University of Aarhus, Denmark. The HRESI-MS Q Exactive (Thermo Scientific) was supported by a grant from ANPCYT, PME2011-PPL2-0009, CEQUIBIEM, DQB, FCEN, UBA.

## REFERENCES

[1] R. Cao, W. Peng, Z. Wang, A. Xu, β-carboline alkaloids: Biochemical and pharmacological functions, Curr. Med. Chem., 14 (2007) 479-500.
[2] T.D. Nikam, K.M. Nitnaware, M.L. Ahire, Alkaloids Derived from Tryptophan: Harmine and Related Alkaloids, in: K.G. Ramawat, J.-M. Mérillon (Eds.) Natural Products: Phytochemistry, Botany and Metabolism of Alkaloids, Phenolics and Terpenes, Springer Berlin Heidelberg, Berlin, Heidelberg, 2013, pp. 553-574.
[3] G.M. Olmedo, L. Cerioni, M.M. González, F.M. Cabrerizo, V.A. Rapisarda, S.I. Volentini, Antifungal activity of β-carbolines on Penicillium digitatum and Botrytis cinerea, Food Microbiol., 62 (2017) 9-14.
[4] G.M. Olmedo, L. Cerioni, M.M. González, F.M. Cabrerizo, S.I. Volentini, V.A. Rapisarda, UVA Photoactivation of Harmol Enhances Its Antifungal Activity against the Phytopathogens Penicillium digitatum and Botrytis cinerea, Front. Microbiol., 8 (2017).
[5] M.L. Alomar, F.A. Rasse-Suriani, A. Ganuza, V.M. Coceres, F.M. Cabrerizo, S.O. Angel, In vitro evaluation of beta-carboline alkaloids as potential anti-Toxoplasma agents, BMC Res Notes, 6 (2013) 193.

[6] K. Butzbach, F.A.O. Rasse-Suriani, M.M. Gonzalez, F.M. Cabrerizo, B. Epe, Albumin–Folate Conjugates for Drug-targeting in Photodynamic Therapy, Photochem. Photobiol., 92 (2016) 611-619.
[7] M.M. Gonzalez, M.P. Denofrio, F.S. Garcia Einschlag, C.A. Franca, R. Pis Diez, R. Erra-Balsells, F.M. Cabrerizo, Determining the molecular basis for the pH-dependent interaction between 2'-deoxynucleotides and 9H-pyrido[3,4-b]indole in its ground and electronic excited states, Phys. Chem. Chem. Phys., 16 (2014) 16547-16562.
[8] M.M. Gonzalez, F.A.O. Rasse-Suriani, C.A. Franca, R. Pis Diez, Y. Gholipour, H. Nonami, R. Erra-Balsells, F.M. Cabrerizo, Photosensitized electron transfer within a self-assembled norharmane–2′-deoxyadenosine 5′-monophosphate (dAMP) complex, Org. Biomol. Chem., 10 (2012) 9359-9372.
[9] M.M. Gonzalez, M. Pellon-Maison, M.A. Ales-Gandolfo, M.R. Gonzalez-Baró, R. Erra-Balsells, F.M. Cabrerizo, Photosensitized cleavage of plasmidic DNA by norharmane, a naturally occurring β-carboline, Org. Biomol. Chem., 8 (2010) 2543-2552.
[10] M.M. Gonzalez, M. Vignoni, M. Pellon-Maison, M.A. Ales-Gandolfo, M.R. Gonzalez-Baro, R. Erra-Balsells, B. Epe, F.M. Cabrerizo, Photosensitization of DNA by β-carbolines: Kinetic analysis and photoproduct characterization, Org. Biomol. Chem., 10 (2012) 1807-1819.
[11] M. Vignoni, F.A.O. Rasse-Suriani, K. Butzbach, R. Erra-Balsells, B. Epe, F.M. Cabrerizo, Mechanisms of DNA damage by photoexcited 9-methyl-β-carbolines, Org. Biomol. Chem., 11 (2013) 5300-5309.
[12] M. Vignoni, R. Erra-Balsells, B. Epe, F.M. Cabrerizo, Intra- and extra-cellular DNA damage by harmine and 9-methyl-harmine, J. Photochem. Photobiol. B, 132 (2014) 66-71.
[13] J.G. Yañuk, M.L. Alomar, M.M. Gonzalez, F. Simon, R. Erra-Balsells, M. Rafti, F.M. Cabrerizo, DNA damage induced by bare and loaded microporous coordination polymers from their ground and electronic excited states, Phys. Chem. Chem. Phys., 17 (2015) 12462-12465.
[14] M.M. Gonzalez, F.M. Cabrerizo, A. Baiker, R. Erra-Balsells, A. Osterman, H. Nitschko, M.G. Vizoso-Pinto, β-Carboline derivatives as novel antivirals for herpes simplex virus, Int. J. Antimicrob. Ag., 52 (2018) 459-468.
[15] J.G. Yañuk, M.P. Denofrio, F.A.O. Rasse-Suriani, F.D. Villarruel, F. Fassetta, F.S. García Einschlag, R. Erra-Balsells, B. Epe, F.M. Cabrerizo, DNA damage photo-induced by chloroharmine isomers: hydrolysis versus oxidation of nucleobases, Org. Biomol. Chem., 16 (2018) 2170-2184.
[16] S. Nafisi, M. Bonsaii, P. Maali, M.A. Khalilzadeh, F. Manouchehri, β-Carboline alkaloids bind DNA, J. Photochem. Photobiol. B, 100 (2010) 84-91.
[17] T. Herraiz, D. Gonzalez, C. Ancin-Azpilicueta, V.J. Aran, H. Guillen, beta-Carboline alkaloids in Peganum harmala and inhibition of human monoamine oxidase (MAO). Food. Chem. Toxicol., 48 (2010) 839-845.
[18] D.M. Wood, P.I. Dargan, Chapter 9 - Mephedrone, in: Novel Psychoactive Substances, Academic Press, Boston, 2013, pp. 211-231.
[19] S.J. Stachell, S.A. Stockwell, D.L. Van Vranken, The fluorescence of scorpions and cataractogenesis, Chem. Biol., 6 (1999) 531-539.
[20] M. Leino, 6-Methoxy-tetrahydro-β-carboline and melatonin in the human retina, Exp. Eye Res., 38 (1984) 325-330.
[21] J. Dillon, A. Spector, K. Nakanishi, Identification of β carbolines isolated from fluorescent human lens proteins, Nature, 259 (1976) 422.
[22] T.M. Kutchan, Strictosidine: From alkaloid to enzyme to gene, Phytochemistry, 32 (1993) 493-506.
[23] J. Stöckigt, L. Barleben, S. Panjikar, E.A. Loris, 3D-Structure and function of strictosidine synthase – the key enzyme of monoterpenoid indole alkaloid biosynthesis, Plant Physiol. Bioch., 46 (2008) 340-355.
[24] J. Stöckigt, A.P. Antonchick, F. Wu, H. Waldmann, The Pictet–Spengler Reaction in Nature and in Organic Chemistry, Angew. Chem. Int. Ed., 50 (2011) 8538-8564.
[25] X. Ma, S. Panjikar, J. Koepke, E. Loris, J. Stöckigt, The Structure of *Rauvolfia serpentina* Strictosidine Synthase Is a Novel Six-Bladed β-Propeller Fold in Plant Proteins, Plant Cell, 18 (2006) 907-920.
[26] Q. Chen, C. Ji, Y. Song, H. Huang, J. Ma, X. Tian, J. Ju, Discovery of McbB, an Enzyme Catalyzing the β-Carboline Skeleton Construction in the Marinacarboline Biosynthetic Pathway, Angew. Chem. Int. Ed., 52 (2013) 9980-9984.
[27] A. Aroonsri, S. Kitani, J. Hashimoto, I. Kosone, M. Izumikawa, M. Komatsu, N. Fujita, Y. Takahashi, K. Shin-ya, H. Ikeda, T. Nihira, Pleiotropic control of secondary metabolism and morphological development by KsbC, a butyrolactone autoregulator receptor homologue in Kitasatospora setae, Appl. Environ. Microb., 78 (2012) 8015-8024.
[28] T. Mori, S. Hoshino, S. Sahashi, T. Wakimoto, T. Matsui, H. Morita, I. Abe, Structural Basis for β-Carboline Alkaloid Production by the Microbial Homodimeric Enzyme McbB, Chem. Biol., (2015).
[29] J. Sopková-de Oliveira Santos, J.C. Smith, M. Delaforge, H. Virelizier, C.K. Jankowski, Oxidation of tetrahydro-β-carboline by cytochrome P-450cam, Eur. J. Biochem., 251 (1998) 398-404.
[30] I. Nemet, L. Varga-Defterdarovic, Methylglyoxal-derived β-carbolines formed from tryptophan and its derivates in the Maillard reaction, Amino Acids, 32 (2007) 291-293.
[31] Y. Kanaoka, E. Sato, O. Yonemitsu, Photo-Induced Dehydrogenation of 3,4-Dehydro-β-carboline System, Chem. Ind. (London), (1968) 1250.
[32] F. Tomas Vert, I. Zabala Sanchez, A. Olba Torrent, Acidity constants of harmaline and harmalol in the ground and excited singlet states, J. Photochem., 26 (1984) 285-294.
[33] G. Petroselli, R. Erra-Balsells, P. David Gara, G.M. Bilmes, Photoacoustic and luminescence characterization of nitrogen heterocyclic aromatic UV-MALDI matrices in solution, Photochem. Photobiol. Sci., 11 (2012) 1062-1068.
[34] M. Balón, J. Hidalgo, P. Guardado, M.A. Muñoz, C. Carmona, Acid-base and spectral properties of β-carbolines. Part 2. Dehydro and fully aromatic β-carbolines, J. Chem. Soc., Perkin Trans. 2, (1993) 99-104.
[35] M.L. Alomar, M.M. Gonzalez, R. Erra-Balsells, F.M. Cabrerizo, Comment on "Binding of alkaloid harmalol to DNA: Photophysical and calorimetric approach", J. Photochem. Photobiol. B, (2014) 26-27.
[36] F.A.O. Rasse-Suriani, F.S. García-Einschlag, M. Rafti, T. Schmidt De León, P.M. David Gara, R. Erra-Balsells, F.M. Cabrerizo, Photophysical and Photochemical Properties of Naturally Occurring normelinonine F and Melinonine F Alkaloids and Structurally Related N(2)- and/or N(9)-methyl-β-carboline Derivatives, Photochem. Photobiol., 94 (2018) 36-51.
[37] O.I. Tarzi, M.A. Ponce, F.M. Cabrerizo, S.M. Bonesi, R. Erra-Balsells, Electronic spectroscopy of the β-carboline derivatives nitronorharmanes, nitroharmanes, nitroharmines and chloroharmines in homogeneous media and in solid matrix, Arkivoc, vii (2005) 295-310.
[38] M.M. Gonzalez, M.L. Salum, Y. Gholipour, F.M. Cabrerizo, R. Erra-Balsells, Photochemistry of norharmane in aqueous solution, Photochem. Photobiol. Sci., 8 (2009) 1139-1149.
[39] M.M. Gonzalez, J. Arnbjerg, M. Paula Denofrio, R. Erra-Balsells, P.R. Ogilby, F.M. Cabrerizo, One- and two-photon excitation of β-carbolines in aqueous solution: pH-dependent spectroscopy, photochemistry, and photophysics, J. Phys. Chem. A, 113 (2009) 6648-6656.
[40] F.A.O. Rasse-Suriani, M. Paula Denofrio, J.G. Yañuk, M. Micaela Gonzalez, E. Wolcan, M. Seifermann, R. Erra-Balsells, F.M. Cabrerizo, Chemical and photochemical properties of chloroharmine derivatives in aqueous solutions, Phys. Chem. Chem. Phys., 18 (2016) 886-900.
[41] O.I. Tarzi, R. Erra-Balsells, Effect of chlorine as substituent on the photochemistry and acid-base properties of β-carboline alkaloids, J. Photochem. Photobiol. B, 82 (2006) 79-93.
[42] O.I. Tarzi, R. Erra-Balsells, Photochemistry of the alkaloids eudistomin N (6-bromo-nor-harmane) and eudistomin O (8-bromo-nor-harmane) and other bromo-β-carbolines, J. Photochem. Photobiol. B, 80 (2005) 29-45.
[43] F.M. Cabrerizo, J. Arnbjerg, M.P. Denofrio, R. Erra-Balsells, P.R. Ogilby, Fluorescence quenching by oxygen: "Debunking" a classic rule, ChemPhysChem, 11 (2010) 796-798.
[44] M. Vignoni, F.M. Cabrerizo, C. Lorente, A.H. Thomas, New Results on the Photochemistry of Biopterin and Neopterin in Aqueous Solution, Photochem. Photobiol., 85 (2009) 365-373.
[45] S.R. Meech, D. Phillips, Photophysics of some common fluorescence standards, J. Photochem., 23 (1983) 193-217.
[46] C. Martí, O. Jürgens, O. Cuenca, M. Casals, S. Nonell, Aromatic ketones as standards for singlet molecular oxygen O2(1Δg) photosensitization. Time-resolved photoacoustic and near-IR emission studies, J. Photochem. Photobiol. A, 97 (1996) 11-18.

[47] T. Ohno, Fluorescence Inner-Filtering Correction for Determining the Humification Index of Dissolved Organic Matter, Environ. Sci. Technol., 36 (2002) 742-746.
[48] S.M. Reed, M.-T. Do, S.E. Masta, Parallel factor analysis of spider fluorophores, J. Photochem. Photobiol. B, 93 (2008) 149-154.
[49] M. Bahram, R. Bro, C. Stedmon, A. Afkhami, Handling of Rayleigh and Raman scatter for PARAFAC modeling of fluorescence data using interpolation, J. Chemom., 20 (2006) 99-105.
[50] A. Pardo, D. Reyman, J.M.L. Poyato, F. Medina, Some β-carboline derivatives as fluorescence standards, J. Lumin., 51 (1992) 269-274.
[51] R.S. Becker, L.F.V. Ferreira, F. Elisei, I. Machado, L. Latterini, Comprehensive photochemistry and photophysics of land- and marine-based β-carbolines employing time-resolved emission and flash transient spectroscopy, Photochem. Photobiol., 81 (2005) 1195-1204.

## GRAPHICAL ABSTRACT

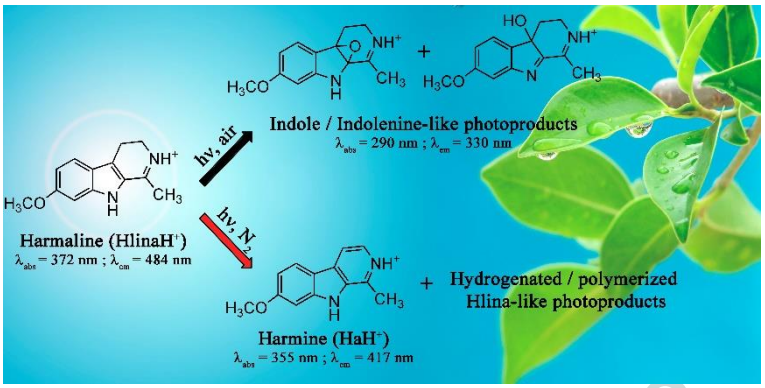


Upon photoexcitation harmaline alkaloid shows a distinctive photochemical behavior modulated by pH and oxygen partial pressure.

1) Harmaline, a partially hydrogenated βC alkaloid, shows a quite distinctive photophysic and photochemical behaviour.
2) Photosensitized formation of reactive oxygen species by photoexcited harmaline is rather small or null.
3) Oxygen partial pressure and pH strongly modulate the photochemical properties of harmaline.
4) Under anaerobic conditions, photoexcited harmaline gives rise to the formation of the full-aromatic βC, harmine.
5) Light might promote additional pathways for the in vivo synthesis and/or photochemical modification of endogenous βCs.

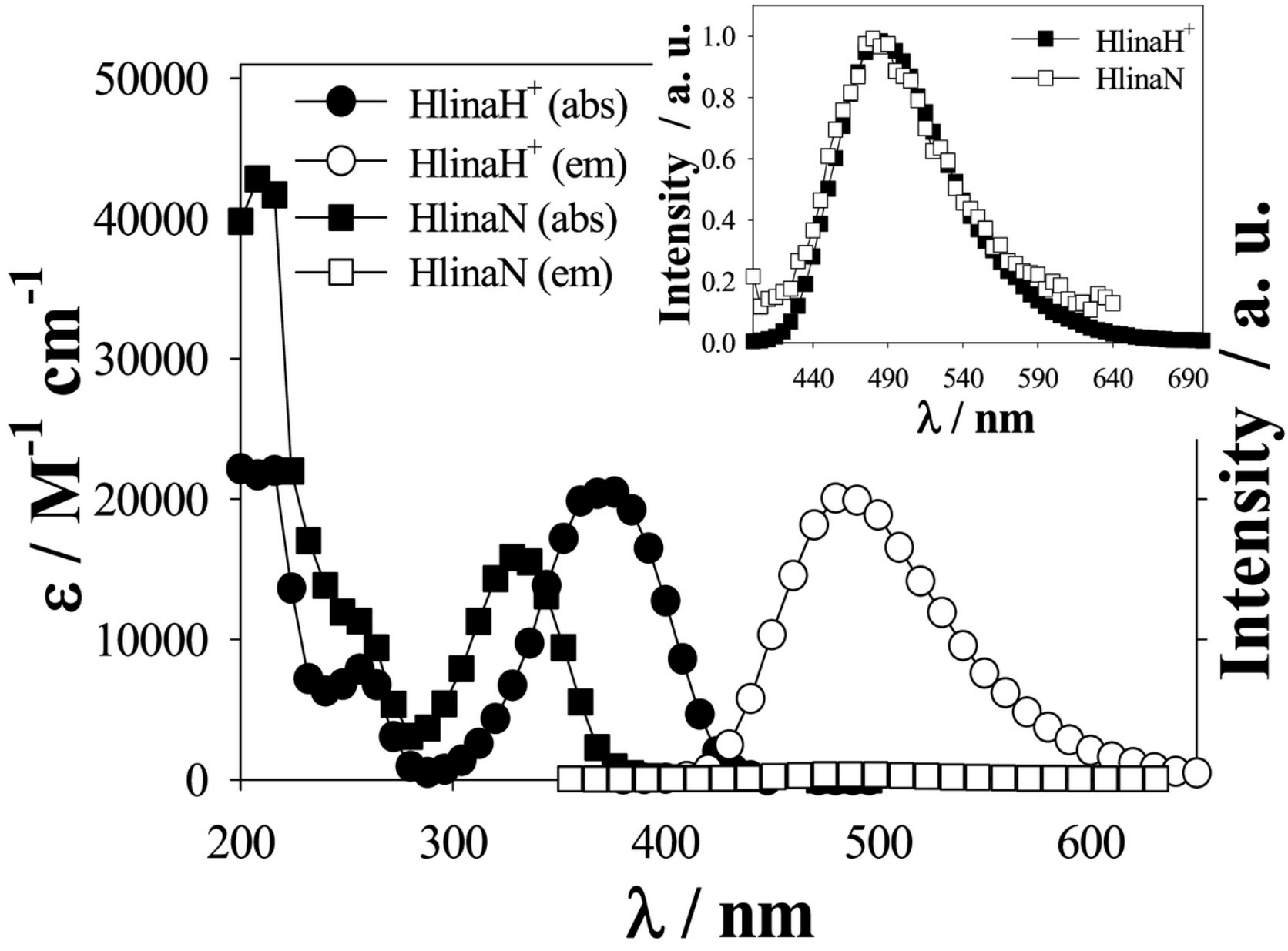
HlinaH+ (abs)
HlinaH+ (em)
HlinaN (abs)
HlinaN (em)
ε / M-1 cm-1
Intensity / a. u.
λ / nm
50000
40000
30000
20000
10000
0
200
300
400
500
600
HlinaH+
HlinaN
1.0
0.8
0.6
0.4
0.2
0.0
440
490
540
590
640
690

Figure 1

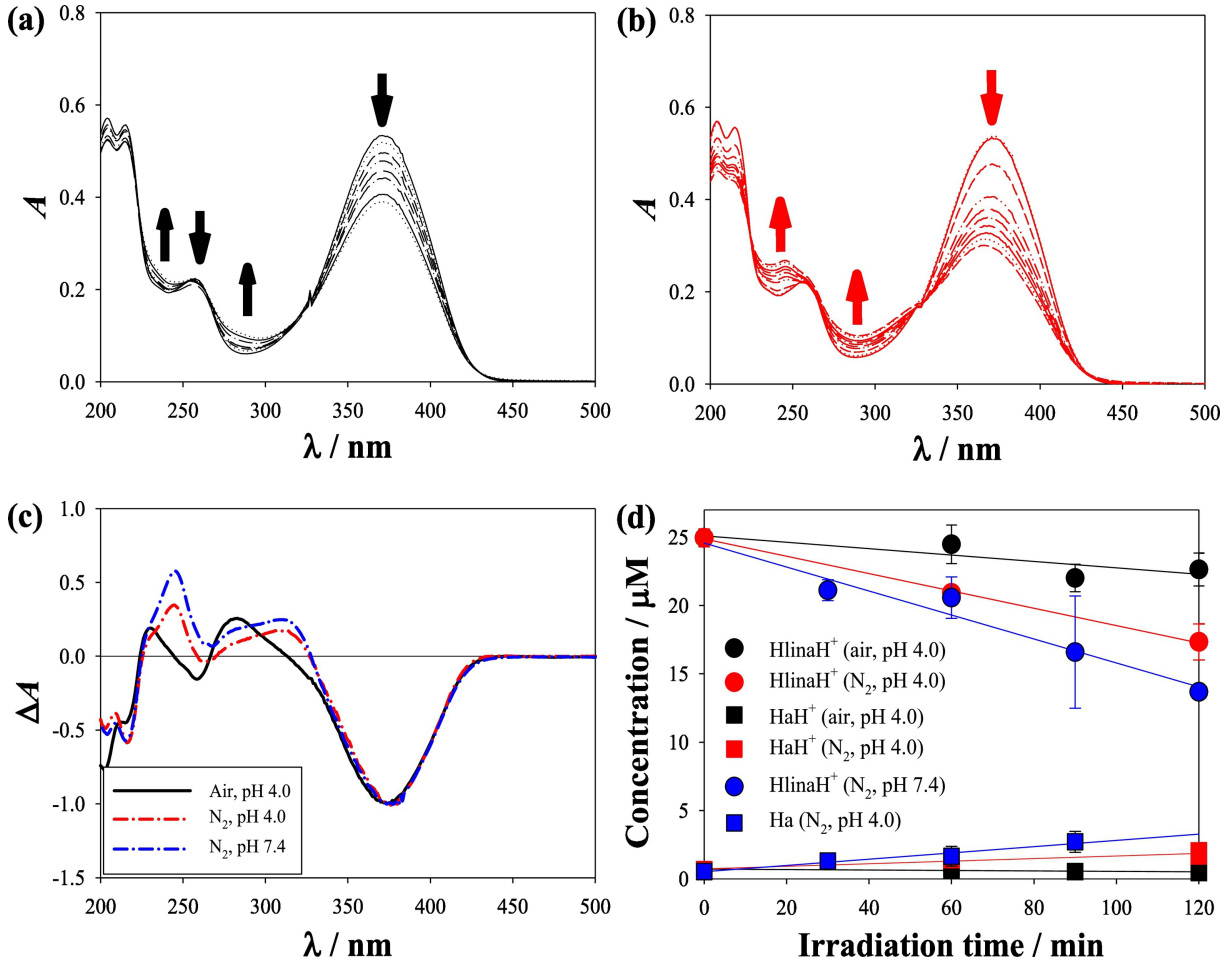
(a)
(b)
(c)
(d)
A
λ / nm
ΔA
Concentration / μM
Irradiation time / min
Air, pH 4.0
N2, pH 4.0
N2, pH 7.4
HlinaH+ (air, pH 4.0)
HlinaH+ (N2, pH 4.0)
HaH+ (air, pH 4.0)
HaH+ (N2, pH 4.0)
HlinaH+ (N2, pH 7.4)
Ha (N2, pH 4.0)

Figure 2

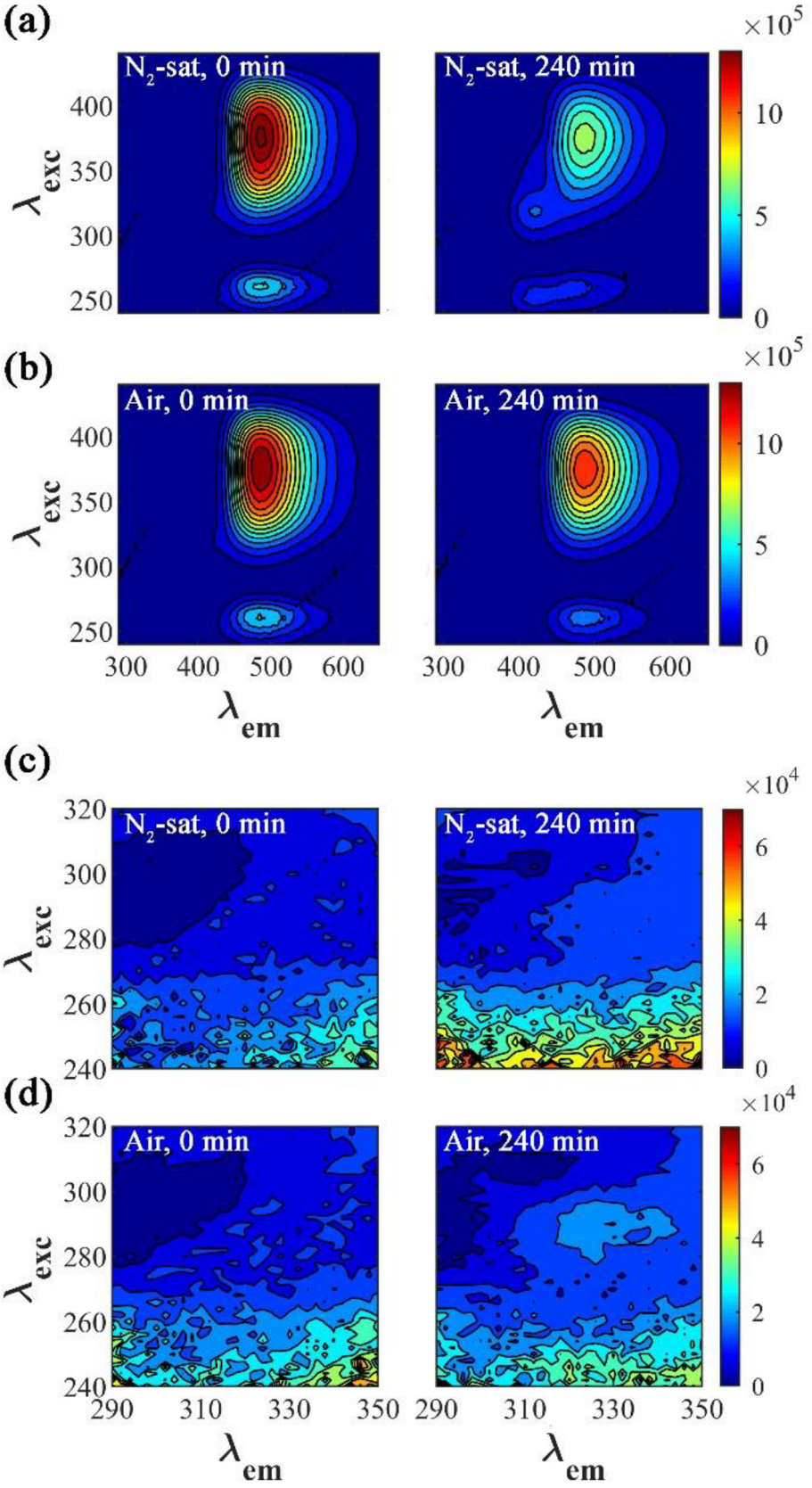
(a)
N2-sat, 0 min
N2-sat, 240 min
×10^5
10
5
0
λexc
400
350
300
250
(b)
Air, 0 min
Air, 240 min
×10^5
10
5
0
300
400
500
600
λem
(c)
N2-sat, 0 min
N2-sat, 240 min
×10^4
6
4
2
0
320
300
280
260
240
(d)
Air, 0 min
Air, 240 min
×10^4
290
310
330
350

Figure 3

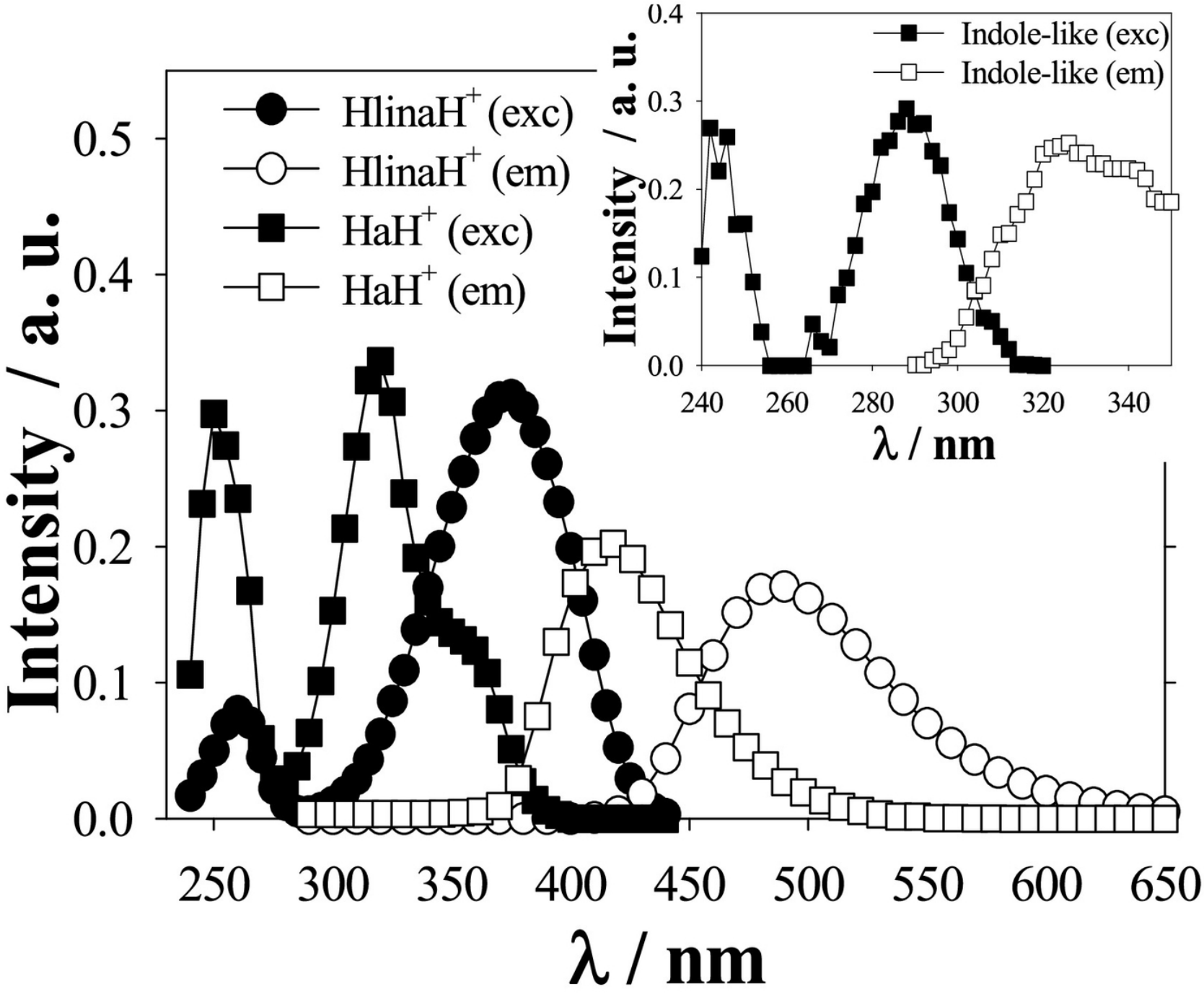
HlinaH+ (exc)
HlinaH+ (em)
HaH+ (exc)
HaH+ (em)
Intensity / a. u.
λ / nm
Indole-like (exc)
Indole-like (em)
Intensity / a. u.
λ / nm

Figure 4

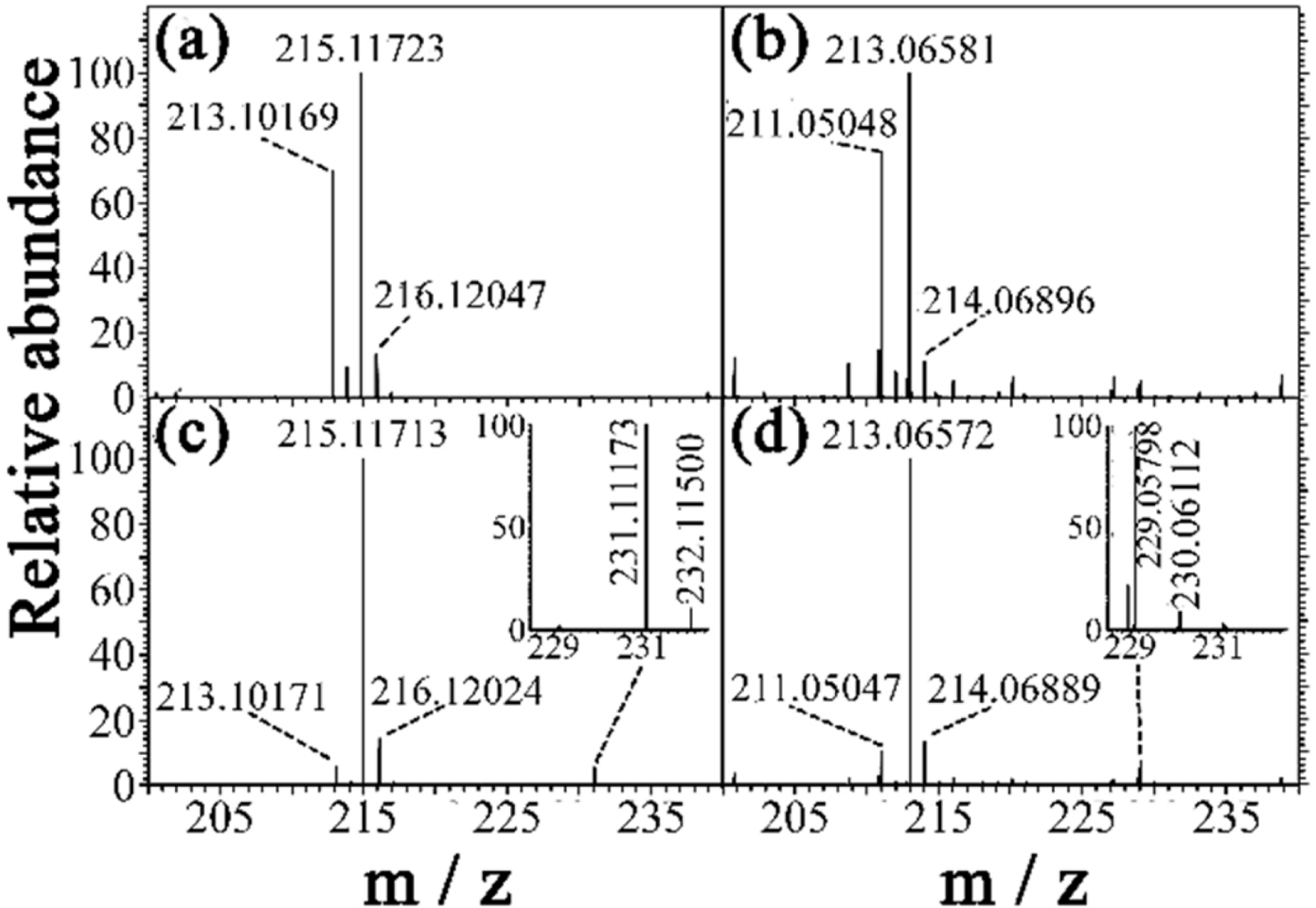
(a)
215.11723
213.10169
216.12047
(b)
213.06581
211.05048
214.06896
(c)
215.11713
231.11173
232.11500
213.10171
216.12024
(d)
213.06572
229.05798
230.06112
211.05047
214.06889
Relative abundance
m / z
m / z

Figure 5